THE JOURNAL OF PHYSICAL CHEMISTRY B

Article

pubs.acs.org/JPCB

Derivation of Coarse Grained Models for Multiscale Simulation of Liquid Crystalline Phase Transitions

Biswaroop Mukherjee,[†] Luigi Delle Site,[‡] Kurt Kremer,*[,†] and Christine Peter*[,†]

[†]Max-Planck-Institut für Polymerforschung, Ackermannweg 10, 55128 Mainz, Germany

[‡]Institute for Mathematics, Freie Universität Berlin, Arnimallee 6, D-14195 Berlin, Germany

Supporting Information

ABSTRACT: We present a systematic derivation of a coarse grained (CG) model for molecular dynamics (MD) simulations of a liquid crystalline (LC) compound containing an azobenzene mesogen. The model aims at a later use in a multiscale modeling approach to study liquid crystalline phase transitions that are (photo)induced by the trans/cis photoisomerization of the mesogen. One of the major challenges in the coarse graining process is the development of models that are for a given chemical system structurally consistent with for example an all-atom reference model and reproduce relevant thermodynamic properties such as the LC phase behavior around the state point of interest. The reduction of number of degrees of freedom makes the resulting coarse models by construction state point dependent; that is, they cannot easily be transferred to a range of temperatures, densities, system compositions, etc. These are significant challenges, in particular if one wants to study LC phase transitions (thermally or photoinduced). In the present paper we show how one can systematically derive a CG model for a LC molecule that is highly consistent with an atomistic description by choosing an appropriate state point for the reference simulation. The reference state point is the supercooled liquid just below the smectic-isotropic phase transition which is characterized by a high degree of local nematic order while being overall isotropic. With the resulting CG model it is possible to switch between the atomistic and the CG levels (and vice versa) in a seamless manner maintaining values of all the relevant order parameters which describe the smectic A (smA) state. This model will allow us in the future to link large length scale and long time scale CG simulations of the LC state with chemically accurate QM/MM simulations of the photoisomerization process.

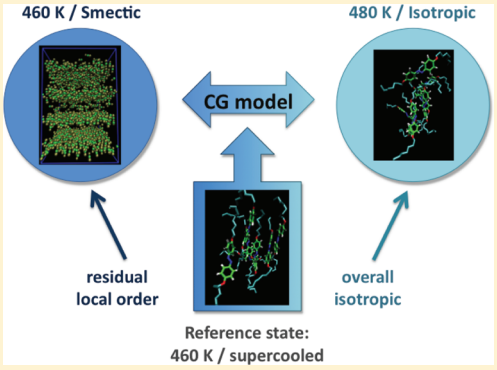

I. INTRODUCTION

Gaining insight into the interesting properties of liquid crystalline (LC) molecules, which are known to self-organize into anisotropic structures, can help us understand a number of systems and phenomena ranging from anisotropic materials to biological self-assembly. To understand liquid crystals and their phase transitions by numerical methods such as molecular dynamics simulations, one needs to study systems of large sizes over long time scales. It is for this reason that models of LC molecules have been minimalistic in their details. From Onsager's calculations[1] we know that generic features like shape anisotropy and excluded volume are sufficient to stabilize a nematic phase above a certain density. Different types of generic models for liquid crystals (both hard and soft, nonspherical particles) have been reviewed by Care and Cleaver.[2] However, these minimal models do have their limitations. For example, they predict too large density changes at the smectic to nematic and the nematic to isotropic transitions,[3,4] and they are often not able to capture properties, e.g., phase transition temperatures, as a function of some chemical detail, like the chain length. Fully atomistic models, on the other hand, are, in principle, capable of reproducing density changes of the correct order of magnitude[5−8] or the coupling between the internal degrees of freedom and the structure of the surrounding fluid.[3] In order to address questions regarding the stability of thermodynamic phases one needs to have access to sufficiently long time and large length scales[9] due to finite size effects and the typical problems associated with first order phase transitions such as hysteresis and metastability. Hence, it is ideal if one can develop models of LC materials which are sufficiently coarse grained (CG) so that mesoscopic time scales become accessible, and on the other hand, also contain sufficient chemical details. To obtain CG models that contain information about the chemical nature of a given molecule and that are capable of correctly reproducing the phases and structures of a specific chemical system, systematic coarse graining approaches have been developed.[10−15] For recent reviews on this subject see refs 16−18. These coarse graining methods are often used in the context of multiscale simulations,

Special Issue: B: Macromolecular Systems Understood through Multiscale and Enhanced Sampling Techniques

Received: December 21, 2011
Revised: March 27, 2012
Published: April 4, 2012

   dx.doi.org/10.1021/jp212300d | J. Phys. Chem. B 2012, 116, 8474−8484

where systems are studied on several levels of resolution, for example a fully atomistic as well as a CG level. In a multiscale simulation ansatz, these levels are systematically connected, so that it is possible to switch back and forth between them. This allows access to the scales necessary to study structure formation of LC phases with the CG level, and after reintroduction of atomistic details, to study the systems also on the level of local interactions. One prerequisite of such an approach is that the two levels are sufficiently consistent. Very often, the interaction functions in the CG model are determined based on atomistic reference simulations. Here different types of reference properties are used as targets in the parametrization process, for example structural properties such as pair correlation functions, i.e., pair potentials of mean force,[19,20] or mean forces, i.e., multidimensional potentials of mean force,[21−23] or thermodynamic properties such as partitioning data.[24−28]

In the present paper we present a structure-based CG model for 8AB8 (see Figure 1), a thermotropic liquid crystal.

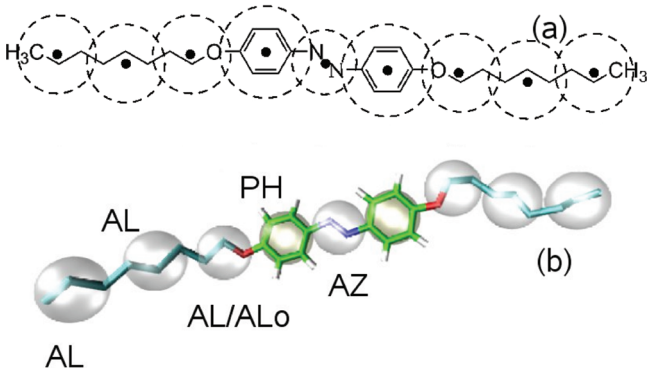

Figure 1. Panel (a) shows the chemical structure of trans 8AB8 and the CG mapping scheme. The different bead types are shown in panel (b). In models I and II (discussed in the text) the 8AB8 molecule is made up of three different types of beads, the AL, PH, and AZ. In model III there is an additional bead type ALo, which describes the two alkyl beads closest to the core of the molecule.

Experimentally, 8AB8 shows a nematic phase between 372 and 385 K and, in addition, a monotropic (only upon cooling) transition from the nematic to a smectic phase.[29] Additionally, the 8AB8 molecules can undergo a photoinduced nematic to isotropic transition which is caused by trans to cis photoisomerization of the azobenzene core. The isomerization results in the change of the shape of the molecule from a straight (in the trans state) to a bent (in the cis state) conformation. The trans molecules favor the formation of the LC phase, whereas the cis molecules tend to disrupt the LC ordering.[30] This effect can be relevant even if only a small fraction of cis molecules is present in the system. The phenomena discussed above span a wide range of length and time-scales from the quantum mechanical (photo isomerization) to the mesoscopic (layer and director undulations in the LC phase) level. It is expected that an ordered LC environment will affect the photoisomerization process of the 8AB8 molecules, which in turn will decide thermodynamic phase of the system. Therefore, a multiscale simulation ansatz that bridges all these phenomena is particularly desirable. It would allow to interchange between simulations at different levels of resolution from a nonadiabatic quantum calculation of the photoisomerization to a CG simulation of the LC phase transition.[31] A key ingredient to such an approach is the development of a CG model which is a faithful representation of a classical atomistic system, which in turn serves as a basis for the QM/MM level. It should be noted that the narrow temperature window of the LC state indicates that rather small details of the interaction play an important role which poses a particular challenge to scale-bridging simulations. This paper deals with the derivation of such a CG model for LC 8AB8 where all the molecules are in the trans configuration. The work is based on an earlier CG model[32] and presents a significant improvement of the agreement with the atomistic reference in terms of structure and phase behavior close to the LC/isotropic phase transition. One does not know beforehand, what should be the choice of CG representation, method of parametrization and also the reference state point at which the coarse graining should be performed. The paper in this context addresses significant questions regarding the coarse graining methodology to study structure formation and phase transitions in complex systems, for example, systems with long-range order. It also addresses general methodological questions regarding the state point transferability of CG models, an issue that has gained an increasing interest in the last years for a variety of systems.[33−40]

The primary idea behind the coarse graining method we present here, is the observation that the short ranged correlations in the ordered phase are not very different from the local correlations present in a disordered phase at suitable thermodynamic state (density, temperature, etc.). It is then possible to construct CG potentials using this disordered phase as the reference state, which then can be used to simulate the ordered phase. In the present context, the chosen reference state is that of a supercooled isotropic liquid with residual short-range LC order. In spirit this procedure is similar to attempts at understanding the freezing transition of several soft matter systems by classical density functional theories.[41−48] Recently, there have been a few attempts at describing lower symmetry phases of complex fluids (molecular crystals, LC nematics) by using potentials derived in the higher symmetry phase (isotropic liquid).[49,50]

The rest of the paper is organized in the following way: Section II briefly discusses the computational details of both atomistic and CG simulations. In section III we investigate the LC phases found in the atomistic reference simulations in order to identify a suitable state point for the multiscale model. In section IV we introduce the structure based coarse graining methodology, where we use the supercooled isotropic liquid as the reference state. Additionally, it is also shown which further refinements to the CG model are necessary in order to achieve a very high level of agreement between atomistic and CG model, so that seamless switching between the two levels of resolution is possible. Section V shows the results obtained with the CG model. By comparing all relevant order parameters, which characterize the LC state, we show that the agreement between CG and atomistic model is very good. With a suitable backmapping procedure atomistic details were reintroduced into conformations obtained from long time scale/large length scale CG simulations, and from these backmapped structures, atomistic, and later QM/MM, simulations can be started that will allow us to study the photoisomerization of 8AB8 in a LC environment.

II. COMPUTATIONAL METHODS

Classical atomistic molecular dynamics simulations were performed with the Gromacs simulation package.[51] For the

dx.doi.org/10.1021/jp212300d | J. Phys. Chem. B 2012, 116, 8474−8484

classical force-field, an adapted version of the (united atom) GROMOS 45a3 force field was used, where the partial charges and parameters of bonded interactions in the azobenzene and the alkoxy linker unit had been (re)parametrized based on quantum-mechanical calculations.[52] The simulations were carried out using a time step of 2 fs and a pressure of 1 bar. Simulations of the reference liquids for parametrization of CG nonbonded potentials were equilibrated at constant pressure, production runs were carried out at constant volume, with the previously determined box size. The weak coupling algorithm was used to control both temperature (coupling constant: 0.1 ps) and pressure (coupling constant was 5.0 ps for isothermal compressibility of 1.0×10^{-5} bar^{-1}).[53] Electrostatic interactions were computed using the Particle Mesh Ewald method,[54] and for Lennard-Jones interactions a twin-range cutoff of 10 and 14 Å (updated every 5 steps) was applied. All chemical bonds were constrained using the LINCS algorithm.[55]

The CG simulations were also performed with the Gromacs simulation package and the iterative Boltzmann inversion (IBI, see section IV) was performed using the tools of the VOTCA package.[56] The simulations were performed in the NVT ensemble (box dimensions obtained from atomistic simulations) using the stochastic dynamics (Langevin) thermostat (coupling time 0.2 ps). We used a time step of 4 fs, and the longest simulation time for the production run was 1000 ns. (Note already here that these are nanoseconds in Lennard-Jones units, not yet accounting for the true speed-up one gets while simulating CG systems. This will be discussed below.) During each iteration of the IBI, the CG system was simulated for 8 ns. We ensured that within this simulation time the molecules moved a distance of at least their own length. For the nonbonded interactions the cutoff was set to 2 nm.

The backmapping was performed in a way discussed in ref 32. After the initial coordinates were generated from the CG snapshot, the structure was relaxed by a series of energy minimization. First, only the atomistic bond potentials and soft-core Lennard-Jones interactions were turned on. Next, all of the bonded interactions (bonds, angles, and dihedrals) were turned on, maintaining soft-core Lennard-Jones interactions. Finally, energy minimization was performed with all interactions. All of the steps were performed with a "virtual site restraint", where an additional harmonic position restraining potential was applied on the atomistic centers so that atoms were forced to match the CG coordinates. After minimization, we performed MD simulations and we heated the system up from 100 to 400 K in steps of 100 K. During this process we gradually increased the time-step from 0.1 to 2 fs. We however maintained the virtual site restraints so that the system could not drift away from the initial CG reference structure. Finally, we simulate the atomistic system at 460 K, without any of the above restraints.

III. ATOMISTIC SIMULATIONS OF LC PHASES OF 8AB8

The CG model we plan to develop aims at studying LC 8AB8 close to the phase transition to the isotropic state in order to be able to also capture the photoinduced phase transition which results from the trans−cis photoisomerization of a fraction of the 8AB8 molecules. For this reason we chose to develop the CG model for the LC system just below the phase transition to the isotropic state. In order to identify this state point, the behavior of the atomistic simulation model needed to be characterized. In an earlier work, long replica exchange simulations had been carried out to this end.[52] It was found that the atomistic model, due to finite size effects, or force field artifacts, or both, does not reproduce the nematic phase and that a smectic phase is observed which undergoes a transition to the isotropic phase around 470 K. A more detailed discussion of the properties of the atomistic model can be found in ref 52. In the present work, short additional calculations at 380, 400, 430, 460, and 480 K were carried out (NPT simulations of 1296 molecules; initial setup of 4 layers of 324 molecules, with the molecules aligned along the z direction of the simulation box) to more carefully characterize the structures in the smectic phase found in the atomistic model, most importantly to differentiate between smectic A and smectic C structures. At each temperature we compute the nematic order parameter S_{nematic}, which is given by the largest eigenvalue of the following tensor:

$$Q_{\alpha\beta} = \frac{1}{N}\sum_{j=1}^{N}\left(\frac{3}{2}u_{j\alpha}u_{j\beta} - \frac{1}{2}\delta_{\alpha\beta}\right) \quad (1)$$

The summation in the above formula is over all N molecules and the unit vector $\boldsymbol{u}_j$ points along the mesogenic core of molecule j. This vector connects the beads denoted by ALo (see Figure 1) on both sides of the core. In addition to S_{nematic}, we also compute the average tilt angle of the macroscopic director (the eigenvector corresponding to the largest eigenvalue) with respect to the layer normal (i.e., the z direction of the simulation box in this case). Figure 2 shows the

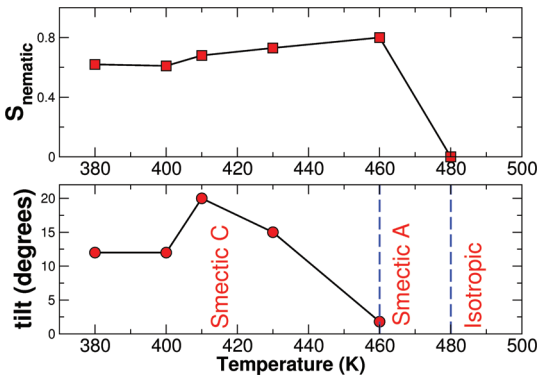

Figure 2. Characterization of LC phases observed in the atomistic model. Panel a shows the average nematic order parameter as a function of temperature. Panel b shows the average tilt angle of the director as function of temperature.

average order parameter and the tilt in the system obtained after simulations of 30 ns at each temperature. Figure 2 shows that at the highest temperature of 480 K the system is in an isotropic state, at 460 K it is in a smA state (data concerning the smectic layering of the system in the *xy* plane of the simulation box are not shown here, but can for example seen in Figure 5), whereas at lower temperatures the system is in the smectic C phase. Please note at this point that this phase diagram is subject to finite size effects and hysteresis, so a comparison with experimental data on 8AB8 should be done with caution. A short discussion regarding the equilibration of the atomistic LC systems can be found in the Supporting Information.

These atomistic simulations serve as a basis to identify a suitable state point for the multiscale model. Since we plan to study LC 8AB8 close to the phase transition, we decided that the CG model should reproduce properties of the atomistic system at 460 K, which is in the smectic A phase. Note

dx.doi.org/10.1021/jp212300d | J. Phys. Chem. B 2012, 116, 8474−8484

however, that this does not imply that we develop the interaction functions of the CG model based on simulations of the *ordered* atomistic system in the smectic A phase at 460 K. The atomistic simulations from which the target properties of the coarse graining process are derived will be discussed in details in the next section.

IV. COARSE GRAINED MODELS FOR 8AB8

A. Mapping Scheme. The mapping scheme, shown in Figure 1, relates the coordinates in the atomistic representation with the bead positions in the CG model. In this work we consider only coarse grained beads with spherically symmetric potentials, and the position of the CG beads is determined by the center of mass of the respective constituting atoms. In the center of the molecule we find the rigid azobenzene mesogen which consists of the two phenyl rings, represented by one bead each (denoted as PH) and the azo bead (AZ) representing the two nitrogen atoms. The two flexible alkyoxy tails consist of three beads each (denoted as AL), for which the bead position is given as the center of mass of the three carbon atoms and in the case of the bead closest to the azobenzene mesogen, the center of mass of the two carbons and the oxygen. Note that in an earlier CG model[32] as well as in the first two models discussed in the present paper the nonbonded interactions involving the three AL beads were treated in the same way; that is, the CG model consists of three types of beads which means that one has to determine six nonbonded interaction potentials in total. In the final model in the present paper we will introduce an additional bead type ALo describing the beads closest to the mesogenic core, including the ether oxygen that links the tail to the phenyl ring. Thus, four bead types imply that we have to determine ten different nonbonded interaction potentials.

B. Derivation of CG Interaction Potentials: Choice of Reference State Point. The bonded interactions of the CG model are derived to reproduce local conformational distributions, i.e., distributions of bond lengths r, bond angles θ, and torsions ϕ between pairs, triples, and quadruples of CG beads respectively. Under the assumption that the bonded and the nonbonded distributions are decoupled and also the internal degrees of freedom are uncorrelated one can factorize the total probability distribution of the internal variables $P^{CG}(r,\theta,\phi,T) = P^{CG}(r,T)P^{CG}(\theta,T)P^{CG}(\phi,T)$. For details about this separation ansatz see, e.g., refs 57 and 58. The distributions can then be Boltzmann inverted to obtain potentials of mean force which can serve as (numerical and tabulated) bond, angle, and torsion interaction functions. In order to obtain a clean separation between bonded and nonbonded interactions, the above distributions should in principle be obtained from the conformational statistics of a single molecule in vacuum (excluding long-range nonbonded interactions along the chain, for details see refs 32, 57, and 58). This, however, relies on the assumption that the (de)coupling between bonded and the nonbonded interactions is the same on atomistic and CG level. In the present case, we found that the distributions of internal degrees of freedom significantly differ between the vacuum sampling and the sampling in the ordered LC state, where the molecules are stretched out due to the LC environment. For this reason we have obtained the bond, angle and dihedral potentials by Boltzmann inversion of the intramolecular distributions of 8AB8 molecules in the smA phase at 460 K. We are aware of the fact that this choice does not cleanly separate the intra- and intermolecular degrees of freedom, leaving a possibility that the same interaction might be accounted for more than once. However, we have confirmed that the particular choice of the method by which the bonded potentials were derived, does not affect the derivation of the nonbonded interactions. The model shows good agreement of molecular conformations on atomistic and CG level (see Figure S13 of the Supporting Information for comparison of the bond distributions obtained from the atomistic and CG model), and we will focus on the derivations of nonbonded interactions from now on.

In the earlier CG model,[32] the nonbonded potentials had been derived from simulations of isotropic liquids of fragments of the 8AB8 molecule, i.e., liquid benzene, azobenzene, octadecane, and various mixtures of these molecules.

The iterative Boltzmann inversion scheme[19] is a numerical procedure to generate a tabulated CG potential that exactly reproduces a given melt structure, like a given radial distribution function $g(r)$. This method relies on an initial guess for a nonbonded potential $U^{CG}_{NB,0}$. The Boltzmann inverse of the target $g(r)$, the potential of mean force

$$U^{CG}_{NB,0} = -k_B T \log g(r) \tag{2}$$

is used, with which one performs a CG simulation of the liquid. The resulting structure of this first step will not match the target structure as the potential of mean force becomes a good estimate of the potential energy only in the limit of infinite dilution. However, on using the following iterative scheme:

$$U^{CG}_{NB,i+1} = U^{CG}_{NB,i} + k_B T \log\left(\frac{g_i(r)}{g(r)}\right) \tag{3}$$

the original guess can be self-consistently refined until the desired structure is obtained.

Originally, this method had been used to generate the CG potentials between molecule fragments in separate simulations of different isotropic liquids or mixtures. However upon closer inspection the phase behavior of the LC state that had been obtained with the fragment based approach was not very satisfactory. The structures obtained with the fragment based CG model are heavily overstructured compared to the smectic atomistic reference. A reparametrization of the CG model while still sticking to the fragment-based ansatz to reproduce the atomistic LC phase behavior better has turned out to be impossible, at least, when following a structure based approach. This drawback of the fragment-based method probably stems from the fact that the packing of the CG units in the liquid of such fragment molecules is different from the packing of the same CG species in the liquid crystalline smA state. One potentially important error one can encounter in the fragment based approach is that different relative orientations between molecule fragments contribute differently to the structure of isotropic liquids of small molecules than to the target liquid or melt, where the fragment is part of a larger molecule which again is "sitting" in a differently ordered environment. Another possible, but probably not as crucial, reason for the above discrepancy is the fact that some partial charges and their effect in determining the structure, which are present at several sites of the molecule in its atomistic description, are not correctly represented in the fragment molecules that are used in the parametrization.

The problems encountered for the fragment based approach are intimately connected to the question of transferability of CG potentials. CG interaction functions are by construction

dx.doi.org/10.1021/jp212300d | J. Phys. Chem. B 2012, 116, 8474−8484

strongly state point dependent, i.e., strictly speaking a CG model is valid only at the state point where it was parametrized, and with state point we here not only refer to temperature and pressure but also to composition of mixtures, molecular environment of a bead, etc. This means transferability of a CG model on the one hand refers to its ability to describe a system at a temperature or pressure which differs from the thermodynamic state point where it had been derived. This is particularly significant here, as this particular work is about describing the various LC phases of the 8AB8 molecule. On the other hand, in the context of a fragment based approach to coarse graining transferability refers to the question whether one can directly transfer the potential derived from the simulation of an isotropic liquid of a particular CG unit to another situation where that unit is either in a mixture with some other species or when it is a part of a longer molecule, like a polymer. The first situation has been previously studied in the context of liquid mixtures.[39,59,60] For benzene water mixtures it has, for example, been shown that potentials obtained by iterative Boltzmann inversion on pure liquid benzene do not favor the benzene aggregation in aqueous solution, which is observed in the atomistic simulations, already at low benzene concentrations.[59] On the other hand, potentials derived from the potential of mean force between two benzene molecules in water correctly describes the system at all concentrations up to demixing − as well as the structure of pure benzene. When a CG bead is a part of a long molecule, like a polymer, then the effective interaction between two CG beads is strongly influenced by the presence of the other parts of the molecules.[57,61] Under such situations the CG interactions can be very successfully derived from simulations of pairs of polymeric chains. This ensures that the presence of neighboring beads is accounted for.

The above observations suggest that fragment based coarse graining is not very suitable to study CG 8AB8 in the smectic phase. Since we want to describe the smA state in the CG description, it would be tempting to perform the iterative Boltzmann inversion on the smA state itself. But this is not possible due to several reasons. The Boltzmann inversion scheme is developed for a system which is isotropic, but in contrast, the smA system is anisotropic. Additionally, the radial distribution functions calculated in the atomistic smA state display long ranged periodicity, with a wavelength equal to the layer spacing of the smectic phase. Iterative Boltzmann inversion on these radial distribution functions will incorporate this periodicity into the CG potential leading to extremely long-ranged, system size dependent potentials. To derive our CG nonbonded potentials, we have followed a philosophy, which is slightly different from the ones that have been followed traditionally in structure based coarse graining. Our method shares some resemblance with classical density functional theories of liquids, which have been quite successful in understanding several problems of soft condensed matter, like freezing of simple and colloidal liquids, glass transition of simple liquids, and phase transitions in liquid crystals.[41−48] The key point behind this class of theories is the observation that the short ranged order in the ordered phase is not very different from that in the disordered phase at a suitable density and temperature. The basic physics lies in the observation that as one approaches the actual phase transition from the high temperature side, the solid state forms due to an instability which occurs in the liquid state. This instability occurs when the correlations in the liquid state exceed a certain critical value. A numerical justification of the above idea emerged during a course of extensive simulation of simple fluids, Hansen and Verlet had observed that the amplitude of the primary peak of the structure factor, $S(k_m)$, is practically constant along the crystallization line, where the liquid coexists with the solid.[62] The grand potential, $\Delta\Omega$, which describes these transitions, has two competing terms,[41] an entropy of disorder (first term in eq 4) favoring the liquid state and an interaction term (second term in eq 4) favoring the solid phase.

$$\frac{\Delta\Omega}{k_B T} = \int d\mathbf{R}\left[\rho(\mathbf{R})\ln\left(\frac{\rho(\mathbf{R})}{\rho_l}\right) - \delta\rho(\mathbf{R})\right] - \frac{1}{2}\int d\mathbf{R}\int d\mathbf{R}'\, c(|\mathbf{R}-\mathbf{R}'|)\delta\rho(\mathbf{R})\delta\rho(\mathbf{R}') + \ldots \quad (4)$$

where $\rho(\mathbf{R})$ is the density at the point $\mathbf{R}$, $\delta\rho(\mathbf{R})$ is $(\rho(\mathbf{R})-\rho_l)$, $c(|\mathbf{R}-\mathbf{R}'|)$ is the direct pair correlation function, T is the temperature, ρ_l is the liquid density, and the dots denotes higher order terms in the correlation functions. In order to study phase transitions, like the one from liquid to solid, the pair correlation function that is used in the above functional is that of an isotropic liquid, of density ρ_l, which coexists with the solid phase. For systems like hard sphere liquids, the correlation function can been obtained from integral equation theories like the Percus−Yevick etc. Alternatively, these correlation functions can also be obtained from either molecular dynamics or Monte Carlo simulations. The goal is to find $\rho(R)$ which minimizes the above functional. There is a trivial solution, $\rho(\mathbf{R}) = \rho_l$, which corresponds to the liquid state, but solutions other than the liquid can exist if $c(|\mathbf{R}-\mathbf{R}'|)$ is sufficiently large. Depending on conditions of average density, temperature and pressure, the stable phase, namely the phase with minimum free energy, can be either a liquid, a solid or even an amorphous state. Reference 63 reviews the different approaches of studying phase transitions by classical density functional methods.

In the present calculation, we have done something which is similar in spirit. We have carried out the iterative Boltzmann inversion and have obtained the potentials on a supercooled, isotropic liquid state at 460 K. Details about the preparation and the equilibration of the supercooled liquid is provided in the Supporting Information. We shall see later that we are able to simulate the smA state quite well using these potentials. This observation then brings up the question as to why does this procedure work. The answer lies in the fact that the liquid state which we have considered for obtaining the nonbonded potentials are structurally "close" to the smA configurations at 460 K. This closeness can be quantified from a correlation function which measures the orientational alignment of nearby molecules. The local nematic ordering[64] can be probed by the quantity

$$g_2(r) = \left\langle \frac{\sum_{i=1}^{(N-1)}\sum_{j=i+1}^{N}\delta(r-|\mathbf{r}_i-\mathbf{r}_j|)P_2(\boldsymbol{u}(\mathbf{r}_i)\cdot\boldsymbol{u}(\mathbf{r}_j))}{\sum_{i=1}^{(N-1)}\sum_{j=i+1}^{N}\delta(r-|\mathbf{r}_i-\mathbf{r}_j|)} \right\rangle \quad (5)$$

where $P_2(x)$ is second order Legendre polynomial and the vectors $\mathbf{u}$ are the same as those used in eq 1. When one performs the coarse graining on these liquids, the effect of these local correlations are built in the potentials. Figure 3 shows the local nematic order calculated from the atomistic trajectories in the smA state at 460 K, isotropic supercooled state at 460 K

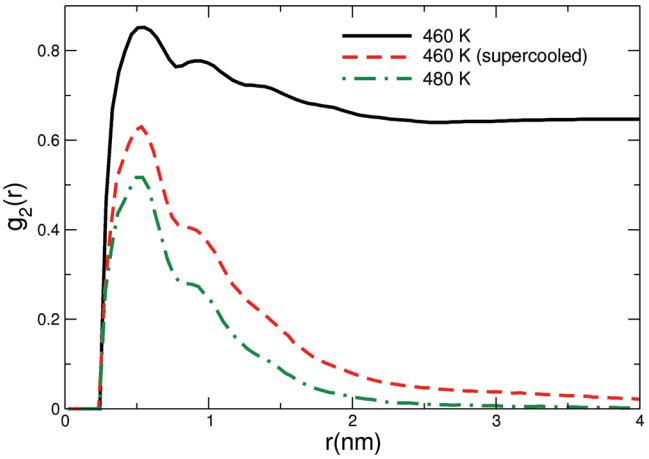

Figure 3. Local nematic order, eq 5 in the text, as a function of separation. This quantity is calculated from the atomistic runs at various temperatures. In the smA phase at 460 K (black, solid line) there is long ranged order present in the system; hence, the correlation function does not decay to zero at large separation. The supercooled, isotropic liquid at 460 K (red, dotted line) and the normal, isotropic liquid at 480 K (green, dash-dotted line) possess some remnant local order, even though the systems on the whole are isotropic. This means that molecules in the first neighboring shell are orientationally ordered. We perform our coarse-graining using the supercooled, isotropic liquid at 460 K as the reference state.

and the isotropic state at 480 K. In the supercooled phase at 460 K, and also at 480 K, there is some remnant local nematic order, even though the system is globally isotropic and the global order parameter vanishes. We decided to parametrize the CG model based on the supercooled liquid at 460 K (i.e., at the temperature where we later intend to carry out the simulations in the ordered LC phase), making use of the slightly increased local order compared to the system at 480 K. In order to make sure that we do not base our CG model on a reference simulation that is transitioning to an ordered state, we have confirmed that this reference system is indeed metastable, i.e., no changes in the structural parameters are observed over time. Details can be found in the Supporting Information.

Before we show results from simulations of 8AB8 at the smA phase with the CG model obtained at the supercooled liquid, we will briefly introduce several small variations of the CG model in order to obtain a very good agreement between the CG and the atomistic simulations at the desired (smA) state point where multiscale simulations are planned in future.

C. Reproducing the Atomistic System, Refining the CG Models. Our primary goal is to obtain a CG model that reproduces the (smA) structure of the LC system near the LC/isotropic phase transition as closely as possible, i.e., accurately enough so that a seamless switching between atomistic and CG simulation level is possible. This is important since ultimately we would like to apply a mixed CG/atomistic/QM approach to understand the mutual influence of 8AB8 photoswitching and the LC phase behavior. The broader implications of such a multiscale calculation is reviewed in ref 31.

While, as we will show below, the above procedure of transferring the model from the reference state point of the supercooled liquid to the ordered smA phase works very well as far as the general phase behavior of the system is concerned, it is to be expected that this transfer will lead to a certain level of deviation between atomistic and CG simulations. However, the outlined multiscale ansatz requires a particularly high level of agreement between CG and atomistic simulations. Switching between CG generated morphologies and atomistic simulations with nonadiabatic QM/MM switching requires agreement of CG and atomistic structures, including the box dimensions in a NPT calculation or the pressure components in a NVT calculation. Preliminary multiscale simulations of photoswitching on backmapped structure have shown that even a small disagreement in pressure components will lead to artifacts in photoswitching due to large forces in the system. For this reason we will present in this section three different models where we slightly vary and progressively improve the derivation of CG potentials and obtain one which describes the smA state best.

- Model I is the model following the approach outlined above without any alterations. This means the 8AB8 molecule is represented by three types of beads (AZ, PH, and AL, i.e., all 6 tail beads are represented by the same bead type). The IBI procedure is started from an initial guess, which is the Boltzmann inversion of the target distribution functions. All of the 6 nonbonded interaction functions are refined iteratively by simulating the supercooled isotropic 8AB8 liquid at 460 K until the respective atomistic target distribution functions are reproduced within error bars.
- Model II is motivated by the observation that in model I the AZ−AZ interaction is very attractive; that is, the interaction between the central beads "carries" most of the structural information. Since the AZ bead is rather buried inside the 8AB8 molecule it appears unphysical that the attraction required to form the observed smectic structures lies practically completely on the AZ−AZ interaction. (We will also see below, that as a result this overstabilizes the smectic layers in the LC phase). In order to prevent this we made in model (II) all the interactions involving the central AZ bead (i.e., AZ−AZ, AZ−PH, and AZ−AL) purely repulsive. This has been done in the way one constructs the WCA potential, by cutting the interactions off in the minimum and shifting the potential to zero at the cutoff (for details see the Supporting Information). The remaining three interactions have then been parametrized using IBI. Note that this also has the advantage of needing to refine fewer potentials in the IBI process, which makes convergence easier, and reduces the probability that the IBI procedure "runs" into an unphysical solution that nevertheless gives a reasonable representation of the global structure. This can happen, in particular for multicomponent systems, in spite of Henderson's theorem[67] which states that there is in principle exactly one numerical solution to this parametrization problem. In practice, however, there are often many, potentially rather different, sets of interaction functions that give a reasonably close representation of the local structure within the error of the radial distribution function.[68]
- Model III accounts for the fact that the six aliphatic tail beads are not of the same chemical type. The two beads which are closest to the core contain an oxygen in the atomistic model and are not exactly equivalent to the four other aliphatic beads. Hence, in this final version we differentiate between the two innermost and the four outermost aliphatic beads (denoted as AL and ALo, see Figure 1). This means that we have now four different

dx.doi.org/10.1021/jp212300d | J. Phys. Chem. B 2012, 116, 8474−8484

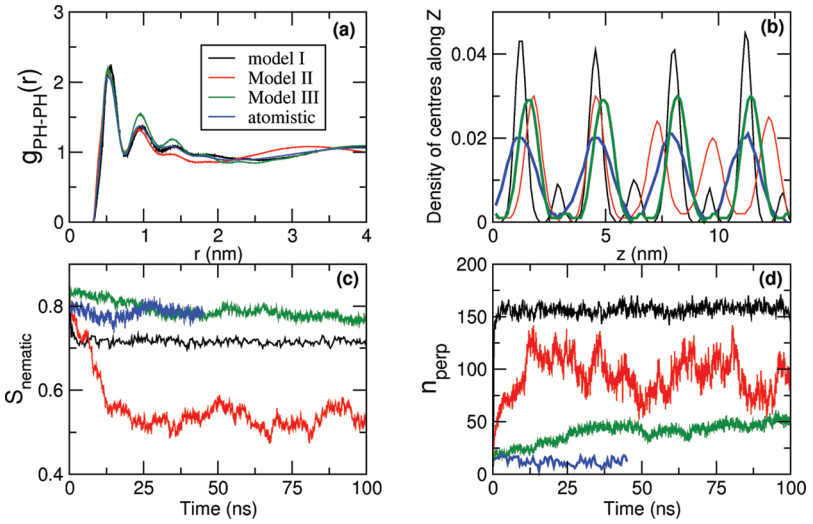

Figure 4. Comparison of the of various quantities calculated in the smectic state of the CG models with the corresponding quantities obtained from the atomistic simulations. Results from model I are denoted in black, model II in red, model III in green and the results from atomistic trajectories are shown in blue. Results from all CG models have been obtained from a 100 ns long trajectory. Atomistic results have been calculated from a 45 ns long trajectory. Panel a shows a comparison of the radial distribution function between the PH beads. Panel b shows the distribution of the centers of the 8AB8 molecules along the z direction (direction perpendicular to the smectic layers). Panel c compares the time evolution of the nematic order parameter. Panel d shows the time series for the evolution of the number of interlayer particles for the three CG and the atomistic models.

types of bead, which in turn, means ten different nonbonded interactions. Of these ten pairs of interactions, the ones involving AZ have been kept repulsive like those in model II. The six remaining interactions have been determined by IBI.

More details about the parametrization of the three models, all interaction functions and comparison of the structures in the CG systems with the atomistic target RDFs (of the supercooled liquid of 8AB8) can be found in the Supporting Information.

V. PROPERTIES OF THE CG MODELS

We simulated the smA state of 8AB8 with the three sets of potentials, starting from a pre-equilibrated atomistic configuration. In all cases, the smA phase was stable and the structure corresponded well to that observed in the atomistic reference simulation, showing that the approach to exploit the residual order in the structure of the supercooled isotropic liquid for parametization worked very well. However for the multiscaling purpose we are aiming at,[31] we require a particularly close structural and thermodynamic correspondence of atomistic and CG model. Therefore we analyze the properties of these CG simulations in the smA phase in more details in the following paragraphs.

Figure 4 shows several structural properties of the LC systems obtained from the three models. Panel a shows the radial distribution function between the centers of mass of the molecules. Panel c shows the time evolution of the nematic order parameter $S_{nematic}$. Both properties show that model III (green lines) agrees best with the atomistic reference. Upon the transition from model I to model II, we observe a loss in structural agreement with the atomistic reference ($S_{nematic}$ is too low, and the long-range tail in the RDF deviates considerably). This is to some extent expected since for model II we deviated from a purely structure-based parametrization of all interaction functions by making some of them entirely repulsive (see above). Why this reparametrization had become necessary in the first place is illustrated in panels b and d. Panel b shows the distribution of the molecule centers in z direction, i.e., the translational order in the direction perpendicular to the smectic layers (averaged over the 100 ns of the CG simulations). We would like to point out that these are nanoseconds in Lennard-Jones units, not yet accounting for the intrinsic speed-up one gets while simulating CG systems. A very rough estimate of this intrinsic speed-up (timescaling factor, for details see ref 65) can be obtained from the ratio of the diffusion coefficients within the smectic layers, i.e., perpendicular to the director, obtained from the atomistic and the coarse grained trajectories $s = D_{CG}/D_{AA}$. We obtained a timescaling factor of about 4 (which comes in addition to the algorithmic speed-up due reduction of resolution). Note that since the smectic state is anisotropic in nature, the timescaling factor for dynamical processes involving motion along the director can be different. A more detailed analysis of the dynamics in the CG LC system will be the subject of a separate study. Figure 4b shows for model I very narrow peaks in the z distribution of the molecule centers; that is, the smectic layers are overstabilized. This pronounced layering is unlike the layering of the atomistic model, where the density peaks are much shorter in height and wider. For model II, where the attraction between the centers of the molecules is lessened, this effect is reduced.

Panel b shows also that for both models I and II we observe a too high (compared to the atomistic reference) probability of finding molecules between the smectic layers. These interlayer molecules lie perpendicular to the macroscopic director. The time-dependence of the number of these interlayer molecules after starting the CG simulations from an atomistically equilibrated configuration is shown in panel d of Figure 4. The presence of a small, but finite number of such interlayer molecules have been observed from the earliest to very recent simulations of the smectic phase.[69,72] For our atomistic 8AB8 system, the number of such molecules is between ten and fifteen (for the present system size of 1296 molecules) and they are distributed uniformly among the four layers. In the CG simulations we not only observe an increasing number of interlayer molecules, we also observe that at long times (beyond ~200 ns) they self-assemble and form an additional

dx.doi.org/10.1021/jp212300d | J. Phys. Chem. B 2012, 116, 8474−8484

"disordered" layer (as can be seen in panel b for model II, for model I this additional layer forms as well, but after much longer simulation times).

Closely associated with the increased number of interlayer molecules, for models I and II, is the observation that the pressure components in x, y, and z directions of the box in a CG NVT simulation with box volume corresponding to the atomistic system, are initially not exactly equal to each other. Table I shows the pressure components in the CG system averaged over the initial 500 ps. The situation of the atomistic and the CG model are very different, when one considers the mean and fluctuations of pressure. Comparing absolute values of pressure obtained from CG and atomistic simulations is meaningless since CG models typically exhibit a high mean pressure if one does not apply a pressure correction.[66] However, one can estimate and compare the pressure anisotropy and the pressure fluctuations of the atomistic and the CG model along (XY plane) and perpendicular to the smectic layers (Z axis). From Table I it is apparent that upon coarse graining the pressure fluctuations, in X and Y directions, are reduced by a factor of ~2, while in the Z direction the reduction is only ~25%.

Table I. Mean and Fluctuations of the Pressure Components during the First 500 ps for the Three CG Models As Discussed in the Text[a]

model	P_{xx} (bar)	P_{yy} (bar)	P_{zz} (bar)	$[(P_{xx} + P_{yy}/2) - P_{zz}]/P_{zz}$(%)
model I	12578 ± 77	12580 ± 76	12182 ± 265	3.3
model II	8232 ± 58	8234 ± 59	7847 ± 249	4.9
model III	8986 ± 57	8990 ± 59	8847 ± 244	1.6
atomistic	7 ± 130	9 ± 130	−1.6 ± 320	

[a]For comparison, also the averages of the atomistic simulation are given. Note that the atomistic model does not have any pressure anisotropy.

In an equilibrated system, the CG smA simulation should exhibit an isotropic pressure, which is also true for the atomistic version of the smA state (last column of Table I). Since in the CG models the pressure components are not equal, the system has to react to the pressure anisotropy, hence the increased number of interlayer molecules. It appears that these LC structures react very sensitively to the pressure anisotropy.

Normally, one would assume that a pressure anisotropy of 3 to 5% is already a very good result and conclude that the correspondence between atomistic and CG models is very good. The small remaining anisotropy could be remedied by a short calculation at constant pressure with a semi-isotropic pressure scaling that allows the box dimensions in x and y direction to adjust independently from the one in z direction. We performed such an equilibration step and found in this case no accumulation of interlayer molecules and formation of additional layers within the simulation box.

However, this is not satisfying in a multiscale study where one wants to reinsert atomistic details into various configurations in the CG trajectory. In that case one does not want to re-equilibrate and readjust box dimensions, and consequentially smectic layer spacing, before starting the photoisomerization simulations. Therefore, the reparametrization of the CG model including the more chemically accurate specific ALo bead (model (III)) had been necessary. Model (III) not only shows the smallest increase of the number of interlayer molecules, i.e. the best agreement with the atomistic reference, for this model we could also run CG simulations starting from a pre-equilibrated atomistic configuration for about 1000 ns (25×10^7 time-steps) without the development of any additional layers. Therefore we have backmapped (reintroduced atomistic coordinates) from various points of the CG run, and compared the structural properties of the CG system and the atomistic system before and after backmapping.

Figure 5 shows the nematic (orientational) order parameter of the system under change of resolution. The initial portion (black curve) is from an atomistic NVT simulation of 20 ns, and then we take the final atomistic snapshot and start the CG simulation from this snapshot. We then run our CG model with our the derived nonbonded potentials (model III). Even during the long runs (25×10^7 time-steps) the structure of the smectic state is preserved very well. The inset in Figure 5 shows the snapshot of the system after the CG model has run sufficiently long. The four well-defined layers are evident. For clarity, only the mesogenic core has been shown. Finally we take the CG snapshot obtained after simulating the CG model for 1000 ns and then backmap it. The blue curve shows the temporal evolution of the nematic order parameter starting from the backmapped structure.

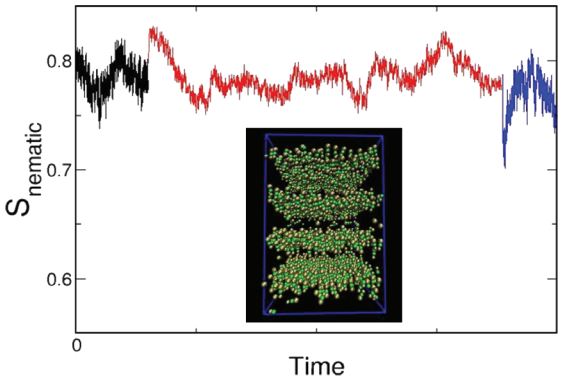

Figure 5. Nematic (orientational) order parameter under change of resolution: The initial portion (black curve) is from an atomistic NVT run of 20 ns, followed by a CG run (red curve) simulated, using model III, for 1000 ns. Finally starting from a configuration obtained by backmapping the final CG configuration, we ran a fully atomistic simulation (blue curve) for 20 ns. There are no units in the time axis because the inherent time-scales in the atomistic and the CG runs are different (see text). The inset shows a snapshot of the system after the CG simulation has run for 500 ns. For clarity, only the three beads at the center of the molecule are shown in the inset. The four smectic layers are apparent.

We have also compared the translational order parameter under this change of resolution. Figure 6 shows the distribution of the molecular center (the AZ bead) for the initial atomistic (black curve), the CG run starting from the atomistic configuration (red curve) and that obtained from an atomistic run which starts from the backmapped structure. The agreement of the rotational and the translational order parameters in the various representations is very good.

VI. CONCLUSIONS AND OUTLOOK

We have presented a systematic derivation of a CG model for LC 8AB8 which aims at a later use in a multiscale modeling approach to study LC phase transitions that are (photo)-induced by the trans/cis photoisomerization of the mesogen.

dx.doi.org/10.1021/jp212300d | J. Phys. Chem. B 2012, 116, 8474−8484

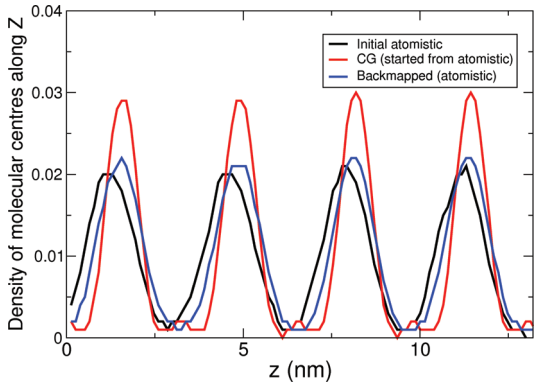

Figure 6. Distribution of the centers of the 8AB8 molecules, along the *Z* direction of the simulation box. The black curve is obtained from an atomistic simulation of duration of 20 ns, followed by a CG run using model III (red curve) of duration 1000 ns. The blue curve is obtained froma an atomistic trajectory which was initiated from a configuration obtained by backmapping the final CG snapshot.

We have specifically addressed the problem of choosing an appropriate reference state point for the parametrization and the aspect of transferability of a CG models across structural changes or phase transitions. The parametrization of the model was done on a supercooled isotropic liquid at a temperature just below the smectic-isotropic phase transition which is characterized by a high local nematic order even though the liquid is isotropic on the whole. The basis for this choice of reference state lies in the more general observation that the local order in the ordered phase is often not very different from that in a disordered phase at a suitable density – an observation which had been made earlier in attempts at understanding the freezing transition of several soft matter systems by classical density functional theories. We find that the so obtained (structure based) CG model is transferable to the ordered LC state and describes the smA structure very well in comparison to an atomistic reference simulation. Furthermore, we have presented a set of refinements to the model for the purpose of a later multiscale (CG/atomistic/QM) simulation approach to study the mutual influence of photoisomerisation and LC phase transition. For this, one requires a CG model which allows a seamless transition between atomistic and CG levels of resolution, i.e. the structural and thermodynamic (for example as far as the pressure components in the system are concerned) agreement between the different models needs to be particularly high. (Note at this point that in order to be able to describe the photoinduced phase transition caused by a certain fraction of cis molecules, we need to ascribe also parameters for the cis molecules. Whether it is possible to represent the cis molecules by the same nonbonded interaction functions as the trans molecules while only modifying the bond, angle and torsion potentials in the central mesogenic unit is currently being tested.) In the refinement process of the CG model for LC 8AB8 we found that several different sets of CG interaction functions give a good representation of the structure of the supercooled liquid and the smA state. Our results suggest that instead of a "pure" structure based CG parametrization, a combination of structural and thermodynamic targets (especially when transferability is important) is more suited in situations where it is necessary to derive CG models which are expected to exhibit phase transitions. It would be very interesting to test this approach toward transferable CG models based on supercooled phases or pretransitional regimes also for other coarse graining methodologies that rely on atomistic reference data such as force matching or related methods.[22] It would be also very interesting to employ other types of coarse graining approaches where the CG potentials are derived from simulations involving isolated pairs of molecules, which have proven to exhibit a remarkable state point transferability for liquids,[70] and see whether the resulting model is able to capture the LC phase transition.

With the CG model it is now possible to simulate larger system sizes and follow them over longer times compared to atomistic simulations. Using the final version of the model we have started to investigate its phase behavior. Preliminary results show that the model both captures the LC to isotropic phase transition upon heating as well as the spontaneous formation of a smectic phase upon cooling down from an isotropic melt. These transitions occur at a temperature window that is in very good agreement with the atomistic model. We have also carried out preliminary investigations of the change of the molecular shape (see the Supporting Information) and the density change at the phase transition. The latter is found to be less than 1%, which compares very well with what is known for low molecular weight liquid crystals,[71] while density changes for generic single site LC models tend to be as high as ∼10%. A more detailed investigation of the phase diagram of the model, including a careful analysis of finite size effects is currently under way. We were also able to perform long simulation (25×10^7 time-steps) on the system of 1296 molecules (the one discussed in this paper). Here, we observe important mechanisms by which relaxation (equilibration) occurs in the smectic phase. In addition to the diffusion of molecules within the smectic layers, we observe that the molecules move from one smectic layer to another. These mechanisms are analogous to those observed recently[72,73] in more generic models (hard spherocylinders) of liquid crystalline molecules. It is important to emphasize that these relaxation mechanisms are rare and it is difficult to observe a significant number of such events in detailed atomistic simulations. It is in these situations, that coarse graining emerges as a really powerful tool to ensure complete (both translational and orientational) equilibration of such complex fluids.

■ ASSOCIATED CONTENT

Supporting Information

Equilibration of the atomistic simulations, and the preparation and structural characterization of the supercooled liquid. Additional information regarding the three types of CG models, including the CG nonbonded potentials. Information on the conformational behavior of the molecules in the atomistic and CG simulations. This material is available free of charge via the Internet at http://pubs.acs.org.

■ AUTHOR INFORMATION

Corresponding Author

*E-mail: kremer@mpip-mainz.mpg.de; peter@mpip-mainz.mpg.de.

Notes

The authors declare no competing financial interest.

■ ACKNOWLEDGMENTS

It is a pleasure to thank C. Junghans, V. Rühle, S. Fritsch, D. Fritz, C. Globisch, A. Debnath, and D. Andrienko for several

discussions and technical help during the course of this work. K. Johnston and D. Mukherji are gratefully acknowledged for a critical reading of this manuscript. We are grateful to the Volkwagen Stiftung for supporting our project within the framework of the program "New Conceptual Approaches to Modeling and Simulation of Complex Systems". C.P. also gratefully acknowledges financial support from the German Science Foundation within the Emmy Noether Program.

REFERENCES

(1) Allen, M. P. *Lect. Notes Phys.* **2006**, *704*, 191−210.
(2) Care, C. M.; Cleaver, D. J. *Rep. Prog. Phys.* **2005**, *68*, 2665−2700.
(3) Wilson, M. R. *Int. Rev. Phys. Chem.* **2005**, *24* (3−4), 421−455.
(4) Brown, J. T.; Allen, M. P.; del Rio, E. M.; de Miguel, E. *Phys. Rev. E* **1998**, *57*, 6685−6699.
(5) Cheung, D. L.; Clark, S. J.; Wilson, M. R. *Phys. Rev. E* **2002**, *65*, 051709.
(6) Cheung, D. L.; Clark, S. J.; Wilson, M. R. *J. Chem. Phys.* **2004**, *121*, 9131−9139.
(7) McDonald, A. J.; Hanna, S. *J. Chem. Phys.* **2006**, *124*, 164906.
(8) Cacelli, I.; De Gaetani, L.; Prampolini, G.; Tani, A. *J. Phys. Chem. B* **2007**, *111*, 2130−2137.
(9) Berardi, R.; Muccioli, L.; Zannoni, C. *ChemPhysChem* **2004**, *5*, 104−111.
(10) Tschop, W.; Kremer, K.; Batoulis, J.; Burger, T.; Hahn, O. *Acta Polym.* **1998**, *49*, 61−74.
(11) Abrams, C. F.; Kremer, K. *Macromolecules* **2003**, *36* (1), 260−267.
(12) van der Vegt, N. F. A.; Peter, C.; Kremer, K. In *Coarse-Graining of Condensed Phase and Biomolecular Systems*; Voth, G. A., Ed.; Chapman and Hall/CRC Press, Taylor and Francis Group: Boca Raton, FL, 2008.
(13) Baschnagel, J.; Binder, K.; Doruker, P.; Gusev, A. A.; Hahn, O.; Kremer, K.; Mattice, W. L.; Müller-Plathe, F.; Murat, M.; Paul, W.; Santos, S.; Suter, U. W.; Tries, V. *Adv. Polym. Sci.* **2000**, *152*, 41−156.
(14) Müller-Plathe, F. *ChemPhysChem* **2002**, *3* (9), 754−769.
(15) Lyubartsev, A.; Mirzoev, A.; Chen, L.; Laaksonen, A. *Faraday Discuss.* **2010**, *144*, 43−56.
(16) *Coarse Graining of Condensed Phase and Biomolecular Systems*; Voth, G. A., Ed.; CRC Press: Boca Raton, FL, 2008.
(17) Peter, C.; Kremer, K. *Faraday Discuss.* **2010**, *144*, 9.
(18) Themed issue on modeling soft matter systems. *Soft Matter*, **2009**, *2* Issue 22.
(19) Reith, D.; Puetz, M.; Müller-Plathe, F. *J. Comput. Chem.* **2003**, *24*, 1624−1636.
(20) Lyubartsev, A.; Laaksonen, A. *Phys. Rev. E* **1995**, *52*, 3730−3737.
(21) Zhou, J.; Thorpe, I.; Izvekov, S.; Voth, G. A. *Biophys. J.* **2007**, *92*, 4289−4303.
(22) Noid, W. G.; Liu, P.; Wang, Y. T.; Chu, J. W.; Ayton, G. S.; Izvekov, S.; Andersen, H. C.; Voth, G. A. *J. Chem. Phys.* **2008**, *128*, 244115.
(23) Mullinax, J. W.; Noid, W. G *Phys. Rev. Lett.* **2010**, *103*, 198104.
(24) Monticelli, L.; Kandasamy, S. K.; Periole, X.; Larson, R. G.; Tieleman, D. P.; Marrink, S. J. *J. Chem. Theory Comput.* **2008**, *4*, 819−834.
(25) Lopez, C. A.; Rzepiela, A. J.; de Vries, A. H.; Dijkhuiezen, L.; Hunenberger, P. H.; Marrinck, S. J. *J. Chem. Theory Comput.* **2009**, *5*, 3195.
(26) DeVane, R.; Shinoda, W.; Moore, P. B.; Klein, M. L. *J. Chem. Theory Comput.* **2009**, *5* (8), 2115−2124.
(27) DeVane, R.; Klein, M. L.; Chiu, C. C.; Nielsen, S. O.; Shinoda, W.; Moore, P. B. *J. Phys. Chem. B* **2010**, *114*, 6386.
(28) Chiu, C. C.; DeVane, R.; Klein, M. L.; Shinoda, W.; Moore, P. B.; Nielsen, S. O. *J. Phys. Chem. B* **2010**, *114*, 6394.
(29) de Jeu, W. H. *J. Phys. (Paris)* **1977**, *38*, 1265−1273.
(30) Lansac, Y.; Glaser, M. A.; Clark, N. A.; Lavrentovich, O. D. *Nature* **1999**, *398*, 54−57.
(31) Boeckmann, M.; Marx, D.; Peter, C.; Delle Site, L.; Kremer, K.; Doltsinis, N. L. *Phys. Chem. Chem. Phys.* **2011**, *13*, 7604−7621.
(32) Peter, C.; Delle Site, L.; Kremer, K. *Soft Matter* **2008**, *4*, 859−869.
(33) Liu, P.; Izvekov, S.; Voth, G. A. *J. Phys. Chem. B* **2007**, *111*, 11566.
(34) Ghosh, J.; Faller, R. *Mol. Simul.* **2007**, *33*, 759.
(35) Qian, H. J.; Carbone, P.; Chen, X.; Karimi-Varzaneh, H. A.; Liu, C. C.; Müller-Plathe, F. *Macromolecules* **2008**, *41*, 9919.
(36) Carbone, P.; Varzaneh, H. A. K.; Chen, X.; Müller-Plathe, F. *J. Chem. Phys.* **2008**, *128*, 064904.
(37) Krishna, V.; Noid, W. G.; Voth, G. A. *J. Chem. Phys.* **2009**, *131*, 024103.
(38) Shen, J. W.; Li, C.; van der Vegt, N. F. A.; Peter, C. *J. Chem. Theory Comput.* **2011**, *7*, 1916−1927.
(39) Mullinax, J. W.; Noid, W. G. *J. Chem. Phys.* **2009**, *131*, 104110.
(40) Engin, O; Villa, A.; Peter, C.; Sayar, M. *Macromol. Theory Simul.* **2011**, *20*, 451−465.
(41) Ramakrishnan, T. V.; Yussouff, M. *Phys. Rev. B* **1979**, *19*, 2775−2794.
(42) Curtin, W. A.; Ashcroft, N. W. *Phys. Rev. Lett.* **1986**, *56*, 2775−2778.
(43) Curtin, W. A. *Phys. Rev. B* **1989**, *39*, 6775−6791.
(44) Rosenfeld, Y. *Phys. Rev. Lett.* **1989**, *63*, 980−983.
(45) Lowen, H. *Phys. Rep.* **1994**, *237*, 249−324.
(46) Singh, Y.; Stoessel, J. P.; Wolynes, P. G. *Phys, Rev. Lett.* **1985**, *54*, 1059−1062.
(47) Poniewierski, A.; Sluckin, T. J. *Phys. Rev. A* **1991**, *43*, 6837−6842.
(48) Jones, R. S.; Ashcroft, N. W. *J. Chem. Phys.* **1984**, *80*, 3328−3335.
(49) Izvekov, S.; Chung, P. W.; Rice, B. M. *J. Chem. Phys.* **2011**, *135*, 044112.
(50) Megariotis, G.; Vyrkou, A.; Leygue, A.; Theodorou, D. *Ind. Eng. Chem. Res.* **2011**, *50*, 546−556.
(51) Hess, B.; Kutzner, C.; van der Spoel, D.; Lindahl, E. *J. Chem. Theory Comput.* **2008**, *4*, 435−447.
(52) Boeckmann, M.; Peter, C.; Delle Site, L.; Doltsinis, N. L.; Kremer, K.; Marx, D. *J. Chem. Theory Comput.* **2007**, *3*, 1789−1802.
(53) Berendsen, H. J. C.; Postma, J. P. M.; van Gunsteren, W. F.; DiNola, A.; Haak, J. R. *J. Chem. Phys.* **1984**, *81*, 3684.
(54) Darden, T.; York, D.; Pedersen, L. *J. Chem. Phys.* **1993**, *98*, 10089−10092.
(55) Hess, H.; Bekker, H.; Berendsen, H.; Fraaije, J. *J. Comput. Chem.* **1997**, *18*, 1463−1472.
(56) Rühle, V.; Junghans, C.; Lukyanov, A.; Kremer, K.; Andrienko, D. *J. Chem. Theory Comput.* **2009**, *5*, 3211−3223.
(57) Fritz, D.; Harmandaris, V. A.; Kremer, K.; van der Vegt, N. F. A. *Macromolecules* **2009**, *42*, 7579−7588.
(58) Bezkorovaynaya, O.; Lukyanov, A.; Kremer, K.; Peter, C. *J. Comput. Chem.* **2012**, *33*, 937−949.
(59) Villa, A.; Peter, C.; van der Vegt, N. F. A. *J. Chem. Theory Comput.* **2010**, *6*, 2434−2444.
(60) Silbermann, J.; Klapp, S. L. H.; Shoen, M.; Channamsetty, N.; Block, H.; Gubbins, K. E. *J. Chem. Phys.* **2006**, *124*, 074105.
(61) McCoy, J. D.; Curro, J. C. *Macromolecules* **1998**, *31*, 9362−9368.
(62) Hansen, J. P.; Verlet, L. *Phys. Rev.* **1969**, *184*, 151−161.
(63) Singh, Y. *Phys. Rep.* **1991**, *207*, No.6.
(64) Cinacchi, G.; De Gaetani, L. *J. Chem. Phys.* **2009**, *130*, 144905.
(65) Fritz, D.; Herbers, C. R.; Kremer, K.; van der Vegt, N. F. A. *Soft Matter* **2009**, *5*, 4556−4563.
(66) Wang, H.; Junghans, C.; Kremer, K. *Eur. Phys. J. E* **2009**, *28*, 221−229.
(67) Henderson, R. L. *Phys. Lett. A* **1974**, *49*, 197−198.
(68) Rzepiela, A. J.; Louhivuori, M.; Peter, C.; Marrink, S. J. *Phys. Chem. Chem. Phys.* **2011**, *13*, 10437−10448.
(69) van Roij, R.; Bolhuis, P.; Mulder, B.; Frenkel, D. *Phys. Rev. E* **1995**, *52*, R1277−R1280.

(70) Brini, E.; Marcon, V.; van der Vegt, N. F. A. *Phys. Chem. Chem. Phys.* **2011**, *13*, 10468−10474.
(71) Wilson, M. R. *Chem. Soc. Rev.* **2007**, *36*, 1881−1888.
(72) Cinacchi, G.; De Gaetani, L. *Phys. Rev. Lett.* **2009**, *103*, 257801.
(73) Patti, A.; El Masri, D.; van Roij, R.; Djikstra, M. *Phys. Rev. Lett.* **2009**, *103*, 248304.